ELSEVIER

11 September 1997

PHYSICS LETTERS B

Physics Letters B 408 (1997) 476–486

Spin-parity analysis of the final state $\pi^+\pi^-\pi^0$ from $\bar{p}p$ annihilation at rest in hydrogen targets at three densities

OBELIX Collaboration

A. Bertin [a], M. Bruschi [a], M. Capponi [a], A. Collamati [a], C. Damiani [a], S. De Castro [a], R. Donà [a], A. Ferretti [a], L. Filippi [a], D. Galli [a], B. Giacobbe [a], U. Marconi [a], I. Massa [a], M. Piccinini [a], M. Poli [a,1], N. Semprini-Cesari [a], R. Spighi [a], V. Vagnoni [a], S. Vecchi [a], A. Vezzani [a], F. Vigotti [a], M. Villa [a], A. Vitale [a], A. Zoccoli [a], M. Corradini [b], A. Donzella [b], E. Lodi Rizzini [b], L. Venturelli [b], A. Zenoni [b], C. Cicaló [c], A. Masoni [c], G. Puddu [c], S. Serci [c], P.P. Temnikov [c], G. Usai [c], O.E. Gorchakov [d], S.N. Prakhov [d], A.M. Rozhdestvensky [d], M.G. Sapozhnikov [d], V.I. Tretyak [d], P. Gianotti [e], C. Guaraldo [e], A. Lanaro [e], V. Lucherini [e], F. Nichitiu [e,2], C. Petrascu [e,2], A. Rosca [e,2], V.G. Ableev [f,3], C. Cavion [f], U. Gastaldi [f], G. Maron [f], R.A. Ricci [f,4], L. Vannucci [f], G. Vedovato [f], G. Bendiscioli [g], V. Filippini [g], A. Fontana [g], P. Montagna [g], A. Rotondi [g], A. Saino [g], P. Salvini [g], C. Scoglio [g], F. Balestra [h], E. Botta [h], T. Bressani [h], M.P. Bussa [h], L. Busso [h], D. Calvo [h], P. Cerello [h], S. Costa [h], O. Denisov [h,3], L. Fava [h], A. Feliciello [h], L. Ferrero [h], A. Filippi [h], R. Garfagnini [h], A. Grasso [h], A. Maggiora [h], S. Marcello [h], D. Panzieri [h], D. Parena [h], E. Rossetto [h], F. Tosello [h], L. Valacca [h], M. Agnello [i], F. Iazzi [i], B. Minetti [i], G. Pauli [j], S. Tessaro [j], L. Santi [k]

[a] *Dip. di Fisica, Univ. di Bologna and INFN, Sez. di Bologna, Bologna, Italy*
[b] *Dip. di Chimica e Fisica per l'Ingegneria e per i Materiali, Univ. di Brescia and INFN, Sez. di Pavia, Pavia, Italy*
[c] *Dip. di Fisica, Univ. di Cagliari and INFN, Sez. di Cagliari, Cagliari, Italy*
[d] *Joint Institute for Nuclear Research, Dubna, Moscow, Russia*
[e] *Laboratori Nazionali di Frascati dell'INFN, Frascati, Italy*
[f] *Laboratori Nazionali di Legnaro dell'INFN, Legnaro, Italy*
[g] *Dip. di Fisica Nucleare e Teorica, Univ. di Pavia, and INFN Sez. di Pavia, Pavia, Italy*
[h] *Dip. di Fisica, Univ. di Torino and INFN, Sez. di Torino, Torino, Italy*
[i] *Politecnico di Torino and INFN, Sez. di Torino, Torino, Italy*
[j] *Istituto di Fisica, Univ. di Trieste and INFN, Sez. di Trieste, Trieste, Italy*
[k] *Istituto di Fisica, Univ. di Udine and INFN, Sez. di Trieste, Trieste, Italy*

Received 21 May 1997; revised manuscript received 18 June 1997
Editor: L. Montanet

PII S0370-2693(97)00791-0

Abstract

The partial wave analysis of the reaction $\bar{p}p \rightarrow \pi^+\pi^-\pi^0$ at rest has been performed for the first time by using high-statistics data sets collected in hydrogen targets at three different densities. The different mixtures of partial waves corresponding to our samples allow a reliable determination of each contribution. This technique is crucial in the identification of the exotic candidate $f_2(1565)$ which can be produced by $^1S_0$, $^3P_1$ and $^3P_2$ initial states. The amplitude analysis was performed in the frame of the K-Matrix and P-Vector approach. It requires the presence of the exotic candidates $f_0(1500)$ and $f_2(1565)$ with the following masses and total widths: (1449 ± 20)MeV, (114 ± 30)MeV and (1507 ± 15)MeV, (130 ± 20)MeV respectively. In addition to $f_0(980)$, $f_0(1300)$ $f_2(1270)$ and $\rho(770)$, a clear evidence of $I = 1$, $J^P = 1^-$ signal, which we identify with $\rho(1450)$, is obtained. © 1997 Published by Elsevier Science B.V.

PACS: 11.80.Et; 11.80.Gw; 13.25; 14.40.Cs

1. Introduction

In the last years an extensive effort has been devoted to the study of $\bar{N}N$ annihilation into three pseudoscalars. At the beginning the main motivation was to clarify the nature of the enhancement in the $\pi\pi$ invariant mass region around 1.5 GeV observed some years before by ASTERIX in P-wave annihilation [1,2]. After the CRYSTAL BARREL measurements in liquid hydrogen [3–5], it became clear that also the S-wave annihilation produces a strong enhancement in the same mass region. The 2^{++} spin-parity assignment [3] initially proposed was consistent with the one of ASTERIX. In more recent analyses [4,5], performed on high statistic samples, two different resonances of comparable mass and different spin-parities (0^{++} and 2^{++}) were identified. It has been suggested that the 0^{++} resonance is the ground state of the scalar glueball [6] predicted by lattice calculations, although to get a clearer evidence on this point, it will be necessary to study its $\bar{K}K$ coupling. As far as the 2^{++} signal is concerned the problem is more controversial. The main difficulty to elucidate its nature is connected to the fact that it is strongly produced in P-wave annihilation, where the only experimental data available so far are those collected by ASTERIX [2]. Further complications arise from the contributions of different atomic states of the $\bar{p}p$ system to the annihilations at rest. As a consequence, a lot of free parameters enter the analysis, whose results become, very often, independently of the statistics, rather unstable. It is clear from the previous considerations that, to get a deeper insight into the details of the resonances produced in the annihilation, it is necessary to have dominant S-wave or P-wave contributions. On the other side, to disentangle in a reliable way each of the involved partial waves, significantly different mixtures of them are needed. In order to get this double goal OBELIX collected $\bar{n}p$ annihilation data in flight from pure $I = 1$ initial state [7,8] and $\bar{p}p$ annihilation data at rest in a wide range of hydrogen densities. It is well known, in fact, that low density favours the radiative de-excitation of $\bar{p}p$ system and therefore P-wave annihilation, while high density induces the Stark-mixing of atomic levels and then S-wave annihilation [9]. Therefore by taking data at different hydrogen target densities, the contributions of the different partial-waves (p.w.) involved can be separated.

In this letter we present the spin-parity analysis of the reaction $\bar{p}p \rightarrow \pi^+\pi^-\pi^0$ at rest. The analysed statistics consist of 1.23×10^6 events collected in liquid hydrogen (LH) and gaseous hydrogen at NTP and at low pressure (5 mbar, LP).

2. Experimental apparatus and data selection

The experiment was carried out on the M2 beam line at the CERN low-energy antiproton ring (LEAR). A description of the OBELIX apparatus can be found elsewhere [10]; here we recall briefly only those features of the apparatus which are necessary to under-

[1] Dip. di Energetica, Univ. di Firenze.

[2] On leave of absence from National Institute of Research and Development for Physics and Nuclear Engineering "Horia Hulubei", Bucharest-Magurele, Romania.

[3] On leave of absence from Joint Institute for Nuclear Research, Dubna, Moscow, Russia

[4] Dipartimento di Fisica, Universita' di Padova and INFN Sezione di Padova, Padova, Italy

stand the present analysis.

The OBELIX spectrometer consists of four subdetectors placed inside the Open Axial Field Magnet which provides a field of 0.5 T. The innermost detector is the Spiral Projection Chamber (SPC), acting as vertex detector with three dimensional readout. The internal cathode consists of a thin aluminized mylar tube which contains the hydrogen gas target. Due to the large size of the LP and LH targets the SPC was used only with NTP gas hydrogen. Around the SPC and coaxially to the beam there are 30 slabs of plastic scintillator which constitute, with a second larger barrel made by 90 scintillator slabs, the time of flight system (TOF). The TOF allows to select (second level trigger) specific multiplicities and topologies of charged particles. Between the two TOF arrays, a cylindrical jet drift chamber (JDC) performs tracking and particle identification by dE/dx measurements. These detectors are finally enclosed by the four supermodules of the high angular resolution gamma detector (HARGD). The $\bar{p}$ beam momentum was 200 MeV/c for the LH target and 105 MeV/c for the NTP and LP ones.

All the experimental data used in the following analysis were collected by requiring an incoming antiproton signal (given by a plastic scintillator in front of the target) and two hits in the internal and external barrels of the TOF (two-prong trigger). To reject the annihilations outside the target suitable time gates were used to select the trigger signal. Pile-up events were discarded on-line. In order to select the $\pi^+\pi^-\pi^0$ final state the following cuts were applied in the off-line analysis:

(i) two recognized tracks of opposite charge in the drift chamber JDC and in the vertex detector SPC (only for the NTP sample);

(ii) a reconstructed vertex in a fiducial volume inside the target;

(iii) an angle between the charged particles which satisfies the following relation:

$$\frac{\boldsymbol{p}_+ \cdot \boldsymbol{p}_-}{|\boldsymbol{p}_+||\boldsymbol{p}_-|} > -0.998 \qquad (1)$$

where $\boldsymbol{p}_+$ and $\boldsymbol{p}_-$ are the momenta of positive and negative particles respectively. This cut rejects, almost totally, the background reactions $\bar{p}p \to \pi^+\pi^-, K^+K^-$;

(iv) a measured dE/dx for the two tracks (obtained by a truncated mean of the energy deposited in the drift cells) within the pion region;

(v) a normalized χ^2 corresponding to a confidence level greater than 5% for the $\pi^+\pi^-\pi^0$ hypothesis both in one-constraint (1C) kinematic fit (by using the measured momenta of the charged prongs) and in 3C fit (by using also the π^0 decay gamma angles measured by HARGD).

The residual background (of the order 15% in 1C data selection) was rejected by an accurate procedure described in Ref. [11], by which we obtain for each measured target density ρ_t a binned (bin size corresponding to 0.0762 GeV$^2/c^4$) background subtracted experimental Dalitz-plot (Dp) $D_E^{jk}(\rho_t)$ (Fig. 1). The number of $\pi^+\pi^-\pi^0$ events obtained in the 1C data selection are: 680.000 (LH), 380.000 (NTP) and 170.000 (LP). The reliability of the background subtraction was checked by comparing the obtained Dp $D_E^{jk}(\rho_t)$ with the background free experimental Dp obtained by 3C data selection (both Dp were corrected for the corresponding acceptance Dp given by events simulated by the OBELIX Monte Carlo code [12]). The full consistency of the two Dp was verified, within the experimental errors, for each measured sample.

In order to have a detailed description of the resolution effects of the apparatus, the acceptance corrections were performed on the binned fit function (theoretical function) by the following linear transformation:

$$D_{T\,\mathrm{acc}}^{jk}(\rho_t) = \sum_{pq} A^{jk,pq}(\rho_t)\, D_T^{pq}(\rho_t) \qquad (2)$$

where $D_{T\,\mathrm{acc}}^{jk}$ is the binned acceptance corrected theoretical Dp and $A^{jk,pq}$ is a multiple array of normalized numbers which represent the efficiency and the apparatus resolution. This transformation map was calculated for each experimental configuration by generating statistics of simulated events greater than the experimental ones.

In the present analysis, besides the three different densities annihilation data also the $I = 0$, S-wave phase shift for $\pi\pi$ elastic scattering obtained by the CERN-Munich collaboration [13] were fitted. The complete χ^2 function minimized by our spin-parity code is defined as follows:

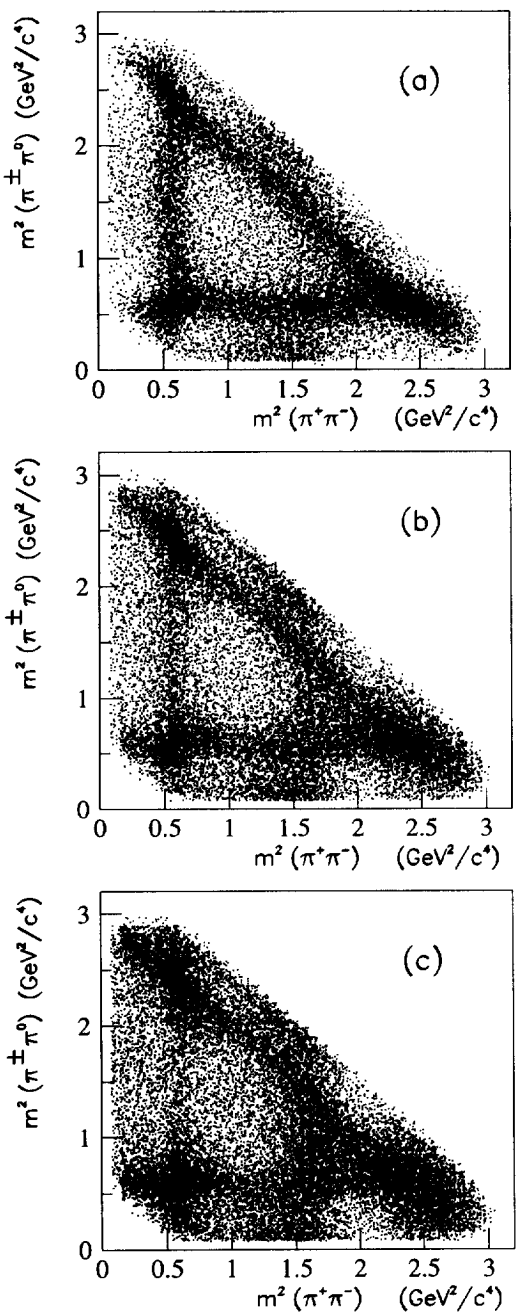

Fig. 1. Dalitz plots (background subtracted and without acceptance corrections) of the reaction $\bar{p}p \to \pi^+\pi^-\pi^0$ from annihilation at rest in liquid hydrogen (a), NTP hydrogen (b) and low pressure hydrogen (c) (two entries per event, each one with weight 0.5).

$$\chi^2 = \sum_{\rho_t} \sum_{jk} \frac{(D^{jk}_{T\,\mathrm{acc}}(\rho_t) - D^{jk}_{E}(\rho_t))^2}{(\epsilon D^{jk}_{T\,\mathrm{acc}}(\rho_t))^2 + (\epsilon D^{jk}_{E}(\rho_t))^2} + W \sum_{j} \frac{(\delta^j_T - \delta^j_E)^2}{(\epsilon\delta^j_E)^2} \quad (3)$$

where $D^{jk}_{T\,\mathrm{acc}}$ and D^{jk}_{E} are the corrected theoretical acceptance and signal Dp respectively, $\epsilon D^{jk}_{T\,\mathrm{acc}}$ and ϵD^{jk}_{E} the corresponding errors, δ^j_T the theoretical phase shift and δ^j_E its experimental value with error $\epsilon\delta^j_E$. The sums run over all the Dp bins of the measured samples (837, 806 and 806 for LH, NTP and LP Dp respectively) and over the experimental points of the phase shift data (33 data points). The weight $W = 15$ is introduced to compensate the large statistical difference between annihilation data ($\sim$ 2400 used cells) and scattering data. Different checks were performed in order to verify the stability of the solutions obtained with different W values.

3. The formalism

We know that, only S and P waves take part to $\bar{p}p$ system annihilation at rest. Among the six hyperfine levels involved, due to parity conservation, the $^3P_0$ cannot produce the three pion final state. Since each p.w. contributes incoherently, we can express the probability density $D_T(\rho_t)$ (in the following we omit the index T) as sum of the squared-modules:

$$D(\rho_t) = \sum f_{^{2S+1}L_J}(\rho_t)\ |A_{^{2S+1}L_J}|^2 \quad (4)$$

Here $f_{^{2S+1}L_J}(\rho_t)$ represents the normalized weight of the corresponding p.w. ($^{2S+1}L_J$ are the quantum numbers of the initial $\bar{p}p$ state) and is the only density depending term. The amplitude $A_{^{2S+1}L_J}$ describes the strong interactions that produce the final state and depend only on the quantum numbers of the p.w. Each measured density introduces in the fit only five new parameters (the weights $f_{^{2S+1}L_J}$) giving on the contrary a number of new constraints of the order of the Dp cells number.

Following the isobar model, the p.w. amplitude $A_{^{2S+1}L_J}$ can be expressed as the sum of two body reactions terms:

$$A_{^{2S+1}L_J} = \sum_{II_3 ll'} C^{II_3}\, Z^{II_3 l', l}_{L}(\boldsymbol{p}, \boldsymbol{q})\, F^{II_3 l'}(q)\, B^{l}(p) \quad (5)$$

Table 1
Isobar quantum numbers and spectator relative angular momenta considered in this analysis

$\bar{p}p$	$^{2S+1}L_J$	$^1S_0$			$^3S_1$	$^1P_1$	$^3P_1$			$^3P_2$	
Isob.	I^G	0^+	0^+	1^+	1^+	1^+	0^+	0^+	1^+	0^+	1^+
	I_3	0	0	±1	$0,\pm1$	$0,\pm1$	0	0	±1	0	±1
	J^{PC}	0^{++}	2^{++}	1^-	1^{--}	1^{--}	0^{++}	2^{++}	1^-	2^{++}	1^-
Spect.	l	0	2	1	1	0,2	1	1	0,2	1	2

Here I and l' are respectively the isospin (I_3 is the third component) and spin of the isobar, l is the isobar-spectator relative angular momentum. The sum runs over all the quantum numbers allowed by selection rules (angular momentum, parity, charge conjugation and isospin conservation). In Table 1 we list the isobars considered in the present analysis. The Clebsch-Gordan coefficients C^{II_3} are crucial in the case of $I = 1$ isobars (in this case it is necessary to order the pions) since they give the correct relative sign, while they can be absorbed in the production amplitude in the other cases. The relative angular momentum between isobar and spectator is represented by the normalized Zemach tensors $Z_L^{II_3l',l}(\boldsymbol{p},\boldsymbol{q})$ [14] where $\boldsymbol{p}$ and $\boldsymbol{q}$ are respectively the spectator momentum (in the laboratory frame) and the decay pion momentum (in the isobar frame). $B^l(p)$ is the Blatt-Weisskopf centrifugal barrier [15] and $F^{II_3l'}(q)$ the isobar relativistic production amplitude which we express in the context of K-Matrix and P-Vector approach [16,17] (we omit the indices) as:

$$F = (I - iK\rho)^{-1} P \tag{6}$$

where I is the identity matrix and ρ the diagonal matrix of two-body phase space. Concerning K-Matrix and P-Vector, we consider $\pi\pi$ ($j = 1$) and $\bar{K}K$ ($j = 2$) couplings for 0^{++} and 2^{++} isobars, and $\pi\pi$ coupling for 1^-. Due to the fact that the $\bar{K}K$ channel is not observed the $\bar{K}K$ coupling includes all the inelastic decay modes. The used expressions are:

$$K_{jl} = \sum_\alpha \frac{g_{\alpha j} g_{\alpha l} B_{\alpha j} B_{\alpha l}}{m_\alpha^2 - m^2} + c_{jl} \tag{7}$$

(8)

$$P_j = \sum_\alpha \frac{\beta_\alpha g_{\alpha j} B_{\alpha j}}{m_\alpha^2 - m^2} \tag{9}$$

Here the sum runs over the considered poles of mass m_α (see below), $B_{\alpha j}$ are connected to Blatt-Weisskopf centrifugal barriers ($B_{\alpha j} = B^{l'}(q)/B^{l'}(q_\alpha)$ where q_α is the resonance breakup momentum) and the production parameters β_α describe the coupling of $\bar{p}p$ system to the resonance. The real constants c_{jl} which parameterize an energy independent component that we call background (in order to distinguish it from the contribution of a resonance) are used only in the 0^{++} isobar. Concerning $g_{\alpha j}$, it describes the coupling of the resonance to final state j ($\pi\pi$ or $\bar{K}K$) and is connected to its partial width $\Gamma_{\alpha j}$ by the formula:

$$g_{\alpha j} = \sqrt{\frac{m_\alpha \Gamma_{\alpha j}}{\rho(m_\alpha)}} \tag{10}$$

By means of the K-Matrix we can construct the transition operator T and the phase-shift corresponding to a given isobar:

$$T = (I - iK\rho)^{-1} K \tag{11}$$

$$\delta_T = \tfrac{1}{2} \arctan\left[\frac{\mathrm{Im}(2i\rho_1 T_{11})}{\mathrm{Re}(2i\rho_1 T_{11} + 1)}\right] \tag{12}$$

The latter expression is used in the present analysis to fit the $\pi\pi$ elastic scattering data. Concerning the production parameters β_α of neutral vector mesons, we considered also the possibility of the electromagnetic mixing. In our case the ω via virtual photon can produce the $\rho^0(770)$ (and viceversa) so we expect the ω contribution in the $\pi^+\pi^-$ invariant mass also if the direct decay into two pions is suppressed [18,19]. To take into account this effect we have modified the production parameters of the $\rho^0(770)$ meson with the following factor:

$$\left(1 + R\,\frac{\delta\,(m_\omega + m_\rho)}{m_\omega^2 - m^2 - i\,m_\omega\,\Gamma_\omega}\right) \tag{13}$$

where δ is the real mixing parameter in the mass matrix of the $\rho - \omega$ system fixed by the partial width of the two pions ω decay [19] (by using the last PDG values

[20] we find $\delta = (2.54 \pm 0.23)$ MeV) and the complex number R is the ratio of ω and $\rho^0(770)$ production parameters ($R = \beta_\omega/\beta_{\rho^0}$) to be determined by the fit.

4. Fit results

In order to insure a good determination of the absolute minimum, each of the physical hypotheses considered was tested by means of a fit strategy tuned on simulated data. First of all we adapted the coefficients β_α and $f_{^{2s+1}L_J}$ taking masses and widths of the resonances fixed to reasonable values. Then after MINUIT convergence we adapted also masses and widths. The two steps were iterated until a good minimum was reached. To be sure to deal with an absolute minimum we compared the solutions obtained by different starting points of the parameters.

The best fit, obtained by including three poles in 0^{++} ($f_0(980)$, $f_0(1300)$, $f_0(1500)$), three poles in 1^- ($\rho(770)$, $\rho(1450)$, $\rho(1700)$) and two poles in 2^{++} isobars ($f_2(1270)$, $f_2(1565)$), gives χ^2/n.d.f. = $3674/(2482-79) = 1.53$ (the n.d.f. is the difference of the total number of experimental data points $837+806+806+33 = 2482$ and the number of free parameters of the fit). No systematic deviations between data and fit are observed in the three Dp, in the corresponding invariant mass projections (Fig. 2) and in the scattering data.

It is not possible to fit correctly the data by using only the $\rho(770)$ in the 1^- isobar. In this case the fit deteriorates (mainly in the LH sample) by $\Delta\chi^2 = 5226$ (compared to the best fit χ^2). Introducing a second pole we obtain a satisfactory description of the data ($\Delta\chi^2 = 16$) with the following resonance parameters: $M = 1330 \pm 40$ MeV, $\Gamma = 690 \pm 30$ MeV. If we try to identify this signal with $\rho(1450)$ we meet a serious difficulty due to the large width obtained by the fit [20]. Our data are compatible with a narrower $\rho(1450)$ only if we include a third pole that we identify with $\rho(1700)$ [22,23]. By fixing mass and width to the PDG values (the fit cannot give a reliable determination of the $\rho(1700)$ parameters due to its position at the boundary of the Dp) we obtain the following $\rho(1450)$ mass and width: $M = 1359 \pm 40$ MeV, $\Gamma = 310 \pm 30$ MeV. Although this three pole solution gives a χ^2 improvement of only 16 units, we consider it as best fit solution since it agrees with the results of $\bar{n}p \to \pi^+\pi^-\pi^+$ [8] and $\bar{p}d \to \pi^-\pi^0\pi^0 p_{\rm spec}$ [21] spin-parity analyses. Concerning $\rho(770)$ we met some difficulties in reproducing correctly the peak shape. We obtained an improvement ($\Delta\chi^2 = 60$ mainly distributed in the $\rho^0(770)$ region) by including in the fit the possibility of $\rho-\omega$ electromagnetic mixing in $^3S_1$ and $^1P_1$ initial states where the selection rules allow $\rho^0(770)$ production.

Table 2
Percentages (normalized to the branching-ratio) of the different partial waves involved in the annihilation at rest in each measured hydrogen density. The uncertainties are obtained by one standard deviation MINUIT errors propagation.

P.W.	LH	NTP	LP
$^1S_0$	17.3 ± 0.8	9.2 ± 0.8	2.7 ± 0.5
$^3S_1$	74.6 ± 1	40.3 ± 2.3	12.2 ± 1.8
$^1P_1$	< 0.3	17.0 ± 3.5	28.5 ± 4
$^3P_1$	2.1 ± 0.6	23.0 ± 1.8	45.3 ± 4
$^3P_2$	6.0 ± 0.5	10.5 ± 0.8	11.3 ± 1.3

Concerning 0^{++} and 2^{++} isobars, we tested the statistical evidence of the signals in the 1.5 GeV mass region by excluding both $f_0(1500)$ and $f_2(1565)$. The obtained χ^2 increase is $\Delta\chi^2 = 1781$. Also in the case we exclude only $f_0(1500)$ or $f_2(1565)$ it is not possible to obtain a satisfactory fit: the χ^2 worsening are $\Delta\chi^2 = 447$ and $\Delta\chi^2 = 292$ respectively.

The non-interfering Dp corresponding to annihilation from each one of the involved p.w. are shown in Fig. 3. By integrating each p.w. over the phase space we calculate their percentage contribution for each measured density (Table 2). Accordingly to the cascade models [9] the S and P wave contributions, although modulated by annihilation dynamics, scale with density: in LH annihilation proceeds almost totally from S-wave while in LP predominant annihilation from P-wave occurs. As far as the hyperfine levels are concerned we find that, within the experimental errors, the percentage ratio of $^3S_1$ and $^1S_0$ is density independent [24]. Concerning the S-wave this fact agrees with the experimental indication that $K_S K_L$ [25] and $\eta(1440)\pi\pi$ [26] b.r. have similar scaling law with density.

The K-Matrix and P-Vector parameters corresponding to the best fit solution are listed in Table 3 (production parameters) and 4 (masses and widths). The $f_0(1500)$ $\pi\pi$ coupling ($\Gamma_{\pi\pi}$) quoted in the Table 4 corresponds to the best fit solution. Nevertheless it is possible, by adapting the production parameters and

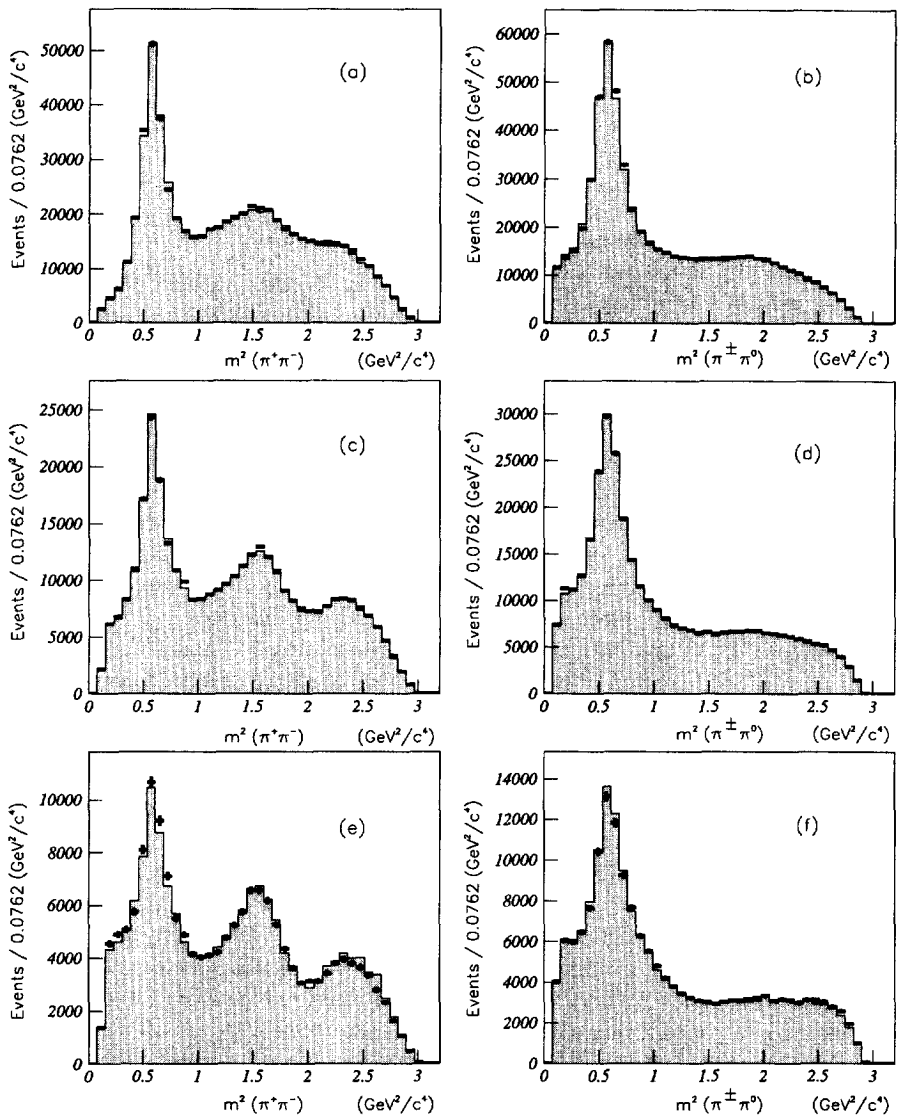

Fig. 2. Fit results (solid line) and experimental data corresponding to the neutral (a,c,e) and charged (b,d,f) $\pi\pi$ invariant mass projections of the Dalitz-plots of the reaction $\bar{p}p \rightarrow \pi^+\pi^-\pi^0$ from annihilation in liquid hydrogen (a,b), NTP hydrogen (c,d) and low pressure hydrogen (e,f). No error bars are included in the fit results.

the partial widths of 0^{++} resonances, to obtain a satisfactory fit (with a slightly worse χ^2) also if the $\Gamma_{\pi\pi}$ value ranges in the interval 0.5–2 MeV. Higher values of this coupling are rejected by χ^2. The nonresonant contribution of 0^{++} K-Matrix isobar (Eq. (8)) determined by the fit has the following value: $c_{12} = 0.80 \pm 0.03$ ($c_{12} = c_{21}$, $c_{11} = c_{22} = 0$). Concerning masses and widths we have to remember that the resonance parameters usually quoted are obtained by looking for singularities of T-Matrix (Eq. (11)) extended in the complex energy plane [17,27]. In our case resonances coupled to $\bar{K}K$ channel and below $\bar{K}K$ threshold correspond to poles in the second Riemann sheet while resonances above this threshold give poles in the third Riemann sheet. The T-Matrix pole parameters corresponding to the best fit solution are shown in Table 4. The position of the $f_0(980)$ pole is essentially determined by scattering data. The mass and

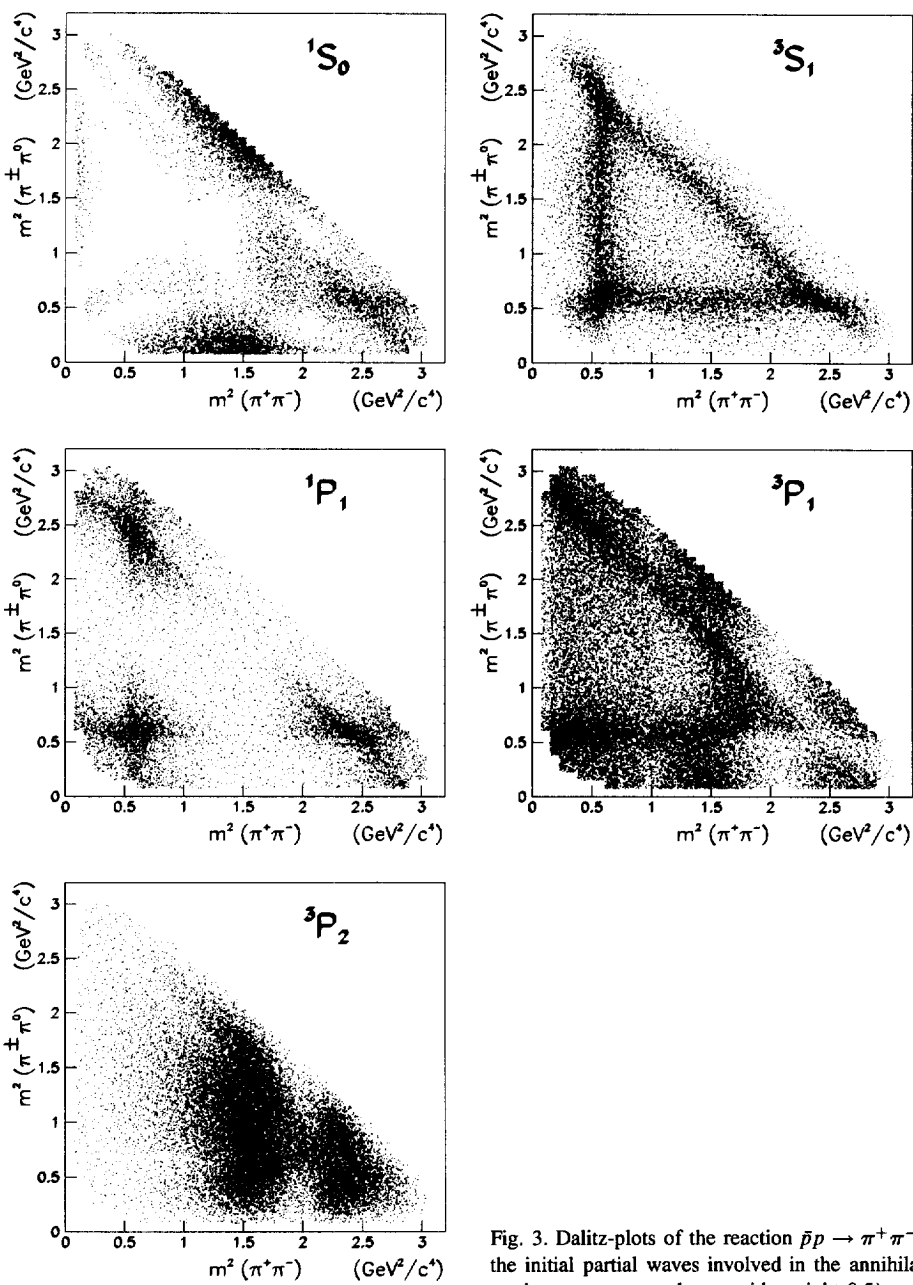

Fig. 3. Dalitz-plots of the reaction $\bar{p}p \to \pi^+\pi^-\pi^0$ from each of the initial partial waves involved in the annihilation at rest (two entries per event, each one with weight 0.5).

width of the resonant state, which correspond to the second Riemann sheet pole agree with existent data [20]. Concerning the second S-wave pole we obtain large values of mass and width in the complex energy plane. Due to the fact that a satisfactory fit of the data is obtained with three S-wave poles, we have not tried to disentangle the broad structure we identify with $f_0(1300)$ in two resonant states by introducing an additional K-Matrix pole. Mass and width of the pole associated to $f_0(1500)$ determined in the present analysis are consistent with the previously measured values [20]. Concerning the $\rho(1450)$ mass and width the agreement with the values obtained by [8] and [21] is satisfactory. As regards the $f_2(1565)$ the mass

Table 3
Real and imaginary part of the production parameters β_α. The one standard deviation MINUIT errors, referred to the last digit, are reported in brackets

Resonance	$^1S_0$	$^3S_1$	$^1P_1$	$^3P_1$	$^3P_2$
$f_0(980)$	0.93(2)	–	–	1.00(1)	–
	−0.29(2)	–	–	0.51(1)	–
$f_0(1300)$	1	–	–	1	–
	0	–	–	0	–
$f_0(1500)$	11.2(2)	–	–	5.5(2)	–
	−3.9(4)	–	–	1.2(3)	–
$\rho(770)$	−1.14(3)	1	1	0.45(3)	−0.044(5)
	0.09(5)	0	0	0.68(3)	−0.039(5)
$\rho(770)_{l=2}$	–	–	1.3(2)	−0.66(3)	–
	–	–	0.3(2)	0.12(2)	–
$\rho(1450)$	−0.28(4)	−0.002(4)	−0.37(10)	−0.05(2)	–
	0.36(2)	−0.070(3)	−0.43(9)	0.14(2)	–
$\rho(1700)$	−0.73(4)	0.14(1)	1.6(2)	−0.29(3)	–
	−0.39(6)	0.023(7)	0.2(2)	0.02(4)	–
$f_2(1270)$	0.94(7)	–	–	0.40(7)	1
	2.30(6)	–	–	2.8(1)	0
$f_2(1565)$	−0.44(10)	–	–	0.01(9)	0.33(3)
	−1.14(9)	–	–	−0.21(10)	−0.89(2)

Table 4
K-Matrix and P-Vector masses and partial widths (columns 1-3) and T-Matrix poles (column 4) of the involved resonances. We quote both the second and the third Riemann sheet poles (first and second row) for $f_0(980)$, second Riemann sheet poles for 1^- isobar and third Riemann sheet poles for the 0^{++} and 2^{++} isobars. The errors listed in the table include also the systematic uncertainties.

Resonance	Mass (MeV)	$\Gamma_{\pi\pi}$ (MeV)	$\Gamma_{\rm All}$ (MeV)	$M - i\,\Gamma/2$ (MeV)
$f_0(980)$	862 ± 4	814 ± 26	0 ± 4	$(994 \pm 9) - i\,(19 \pm 10)$
				$(963 \pm 8) - i\,(29 \pm 10)$
$f_0(1300)$	1257 ± 20	1537 ± 74	73 ± 13	$(1548 \pm 40) - i\,(560 \pm 40)$
$f_0(1500)$	1463 ± 11	1.0 ± 0.2	119 ± 15	$(1449 \pm 20) - i\,(57 \pm 15)$
$\rho(770)$	732 ± 7	150 ± 7	–	$(765 \pm 6) - i\,(61 \pm 10)$
$\rho(1450)$	1303 ± 21	300 ± 20	–	$(1359 \pm 40) - i\,(155 \pm 20)$
$\rho(1700)$	1770	300	–	$(1719 \pm 15) - i\,(155 \pm 20)$
$f_2(1270)$	1260 ± 7	133 ± 9	56 ± 11	$(1278 \pm 5) - i\,(102 \pm 10)$
$f_2(1565)$	1525 ± 11	134 ± 16	0.3 ± 0.3	$(1507 \pm 15) - i\,(65 \pm 10)$

value is slightly low when compared to the last PDG value and to the $\bar{n}p$ analyses results [7,8]. As far as the $\rho - \omega$ mixing is concerned the fit gives the following value for the complex parameter R (Eq. 13) corresponding to $^3S_1$ initial state: $|R| = 0.19 \pm 0.06, \phi_R = -0.5 \pm 0.3$. Assuming that the squared module of R could be connected to the ratio of b.r. of $\bar{p}p$ in $\omega\pi^0$ and $\rho^0\pi^0$ we get a suppression of the ω production with respect to the ρ^0 production from $^3S_1$ initial state annihilation. Due to the large $\rho(770)$ contribution with $l = 2$ (Table 1) in $^1P_1$ initial state the $\rho^0(770)$ signal is suppressed in the central region by Zemach tensor while it is visible in the interference region. For this reason it is difficult to determine the corresponding R value and the fit gives a large error: $|R| = 3 \pm 2, \phi_R = 1.7 \pm 1$.

In general, due to reciprocal interference, it is not possible to give a rigorous meaning to the branching ratios of one of the possible intermediate states from a given initial state. In our case strong interferences occur between all the resonances with the exception of ρ and $f_2(1270)$ where the integrals over the Dp of the interfering terms balance. Nevertheless, to get an idea of the relative strengths of the resonant states,

Table 5
Percentages (normalized to the unit in each partial wave) of the different resonances considered in the present analysis. Interferences between the different resonances are not taken into account (see text for explanation). The uncertainties are obtained by one standard deviation MINUIT errors propagation.

Resonance	$^1S_0$	$^3S_1$	$^1P_1$	$^3P_1$	$^3P_2$
$f_0(980)$	0.3(1)	–	–	2.8(3)	–
$f_0(1300)$	45.2(5)	–	–	53.5(9)	–
$f_0(1500)$	3.8(3)	–	–	0.9(3)	–
$\rho(770)$	11.0(8)	92.8(9)	75.5(7)	22.2(5)	3.5(5)
$\rho(1450)$	1.7(4)	4.2(5)	6.2(6)	0.9(5)	–
$\rho(1700)$	3.8(4)	3.0(5)	18.3(8)	0.8(5)	–
$f_2(1270)$	28.0(3)	–	–	17.8(9)	61.5(5)
$f_2(1565)$	6.2(3)	–	–	1.1(5)	35.0(5)

it is useful to integrate over the Dp each contribution. To obtain quantities related to the different T-Matrix poles we have fitted the amplitude production corresponding to a given isobar as sum of Breit-Wigner shapes and a suitable background term (considered only in the $I = 0$, $J^{PC} = 0^{++}$ isobar amplitude). We obtain values of masses and widths perfectly consistent with the T-Matrix poles. The integration over the phase space of each Breit-Wigner separately gives the values reported in the Table 5 where each p.w. is normalized to the unit. Due to the fact that interferences between different isobars are at most of few percents the sum of the resonance percentages corresponding to the same isobar can be really interpreted as b.r. Of course this is not true for the resonances within the same isobar where strong interference effects occur. From Table 5 we see that the $^1S_0$ and $^3P_1$ initial states show a similar structure with production of 0^{++}, 1^- and 2^{++} resonances. Although $^3S_1$ and $^1P_1$ are dominated by $\rho(770)$ production, $\rho(1450)$ and $\rho(1700)$ signals are observed. The $f_2(1565)$ production from P-wave occurs almost totally from $^3P_2$.

5. Conclusions

The results of spin-parity analysis of the annihilation reaction $\bar{p}p \to \pi^+\pi^-\pi^0$ detected with the same apparatus at rest at three different hydrogen densities are presented for the first time. The simultaneous analysis of the different data samples reduces substantially the ambiguities arising from the contribution of five partial waves in the initial state and allows a reliable assignment of the quantum numbers to the observed signals. This is possible also when a partial wave contribution is weak like in the case of P and S-wave annihilation in liquid and low pressure hydrogen respectively. This technique is crucial in the identification of the exotic candidate $f_2(1565)$ which can be produced by $^1S_0$, $^3P_1$ and $^3P_2$ initial states. Mass and total width are (1507 ± 15) MeV and (130 ± 20) MeV respectively. The $I = 0$, $J^{PC} = 0^{++}$ amplitude is well fitted by a three pole solution and a constant term in K-matrix. The exotic candidate $f_0(1500)$, identified for the first time in this final state, is produced by $^1S_0$ and $^3P_1$ partial waves and its mass and total width turn out to be (1449 ± 20) MeV and (114 ± 30) MeV respectively. Clear evidence of $I = 1$, $J^P = 1^-$ signal from $^1S_0$, $^3S_1$, $^1P_1$ and $^3P_1$ is obtained. This signal which we identify with $\rho(1450)$ is observed in three charged states. In the selected solution (where mass and width of the $\rho(1700)$ are fixed by PDG values [20]) mass and total width are determined to be (1359 ± 40) MeV and (310 ± 40) MeV respectively. An improvement of the fit in the $\rho(770)$ region is obtained by considering $\rho - \omega$ mixing. The percentages of the partial waves contributions are determined in all the measured densities and the $^3S_1/^1S_0$ ratio turns out to be density independent. The goals reached by the present analysis consist in the identification of the quantum numbers, masses total widths and $\pi\pi$ couplings of the resonances involved in the production of the final state $\pi^+\pi^-\pi^0$. A progress in the understanding of the nature of the exotic candidates $f_0(1500)$ and $f_2(1565)$ will be possible by measuring also the $\bar{K}K$ couplings. For this purpose OBELIX has collected consistent statistics of $\bar{p}p$ annihilations in the final state $\bar{K}K\pi$ in different hydrogen target densities.

References

[1] Asterix Collab., B. May et al., Z. Phys. C 46 (1990) 191.
[2] Asterix Collab., B. May et al., Z. Phys. C 46 (1990) 203.
[3] Crystal Barrel Collab., E. Aker et al., Phys. Lett. B 260 (1991) 249.
[4] Crystal Barrel Collab., C. Amsler et al., Phys. Lett. B 323 (1994) 233.
[5] Crystal Barrel Collab., C. Amsler et al., Phys. Lett. B 342 (1995) 433.
[6] C. Amsler, F.E. Close, Phys. Rev. D 53 (1996) 295.
[7] A. Adamo et al., Nucl. Phys. A 558 (1993) 13c.
[8] Obelix Collab., A. Bertin et al., submitted to Phys. Rev. D.
[9] G. Reifenrother, E. Klempt, Nucl. Phys. A 503 (1989) 885.

[10] Obelix Collab., A. Adamo et al., Sov. J. Nucl. Phys. 55 (1992) 1732.
[11] Obelix Collab., V.G. Ableev et al., in: LEAP '94, Proceedings of the Biennial Conference on Low-Energy Antiproton Physics, Bled, Slovenia, ed. G. Kernel et al., p. 130.
[12] R. Brun et al., GEANT 3, Internal Report CERN DD/EE/84-1, CERN, 1987.
[13] G. Grayer et al., Nucl. Phys. B 75 (1974) 189.
[14] C. Zemach, Phys. Rev. 133 (1964) 1201. Phys. Rev. 140 (1965) 97. Phys. Rev. 140 (1965) 109.
[15] F.V. Hippel and C. Quigg, Phys. Rev. D 5 (1972) 624.
[16] I.J. Aitchinson, Nucl. Phys. A 189 (1972) 417.
[17] S.U. Chung et al., Ann. Physik 4 (1995) 404.
[18] S. Coleman and H.J. Schnitzer, Phys. Rev. 134 (1964) 863. A.S. Goldhaber, C.G. Fox and C. Quigg, Phys. Lett. B 30 (1969) 249. N.N. Achasov et al. Intern. J. Mod. Phys. A 7 (1992) 3187.
[19] Asterix Collab., P. Weidenauer et al., Z. Phys. C 59 (1993) 387.
[20] Review of Particle Properties, Phys. Rev. D 54 (1996) .
[21] Crystal Barrel Collab., A. Abele et al., Phys. Lett. B 391 (1997) 191.
[22] A.B. Clegg and A. Donnachie, Z. Phys. C 62 (1994) 455.
[23] A. Donnachie, Y.S. Kalashnikova and A.B. Clegg Z. Phys. C 60 (1993) 187.
[24] C. Batty, Nucl. Phys. A 601 (1996) 425.
[25] Obelix Collab., A. Bertin et al., Phys. Lett. B 386 (1996) 486.
[26] Obelix Collab., A. Bertin et al., Phys. Lett. B 385 (1996) 383.
[27] A.M. Badalyan, L.P. KOK, M.I. Polikarpov and Y.A. Simonov, Phys. Lett. B 82 (1982) 31.